Chinese Chemical Letters 34 (2023) 108002

Contents lists available at ScienceDirect

Chinese Chemical Letters

journal homepage: www.elsevier.com/locate/cclet

Light-driven interconversion of Pd_2L_4 cage and mononuclear PdL_2 mediated by the isomerization of azobenzene ligand

Jinkang Zhu, Xujin Chen, Xin Jin, Qiaochun Wang*

Key Laboratory for Advanced Materials, Joint International Research Laboratory of Precision Chemistry and Molecular Engineering, Feringa Nobel Prize Scientist Joint Research Center, Frontiers Science Center for Materiobiology and Dynamic Chemistry, Institute of Fine Chemicals, School of Chemistry and Molecular Engineering, East China University of Science and Technology, Shanghai 200237, China

ARTICLE INFO

Article history:
Received 30 August 2022
Revised 4 November 2022
Accepted 10 November 2022
Available online 12 November 2022

Keywords:
Molecular cage
Azobenzene
Isomerization
Pd_2L_4
PdL_2

ABSTRACT

The lantern-shaped cage Pd_2L_4 and tweezer-like PdL_2 can be synthesized from the *trans*- and *cis*-isomer of an azobenzene-containing ligand, respectively, which were characterized by ^1H, ^{13}C, ^1H-^1H COSY, DOSY NMR spectroscopies, high-resolution ESI-MS and density function theory (DFT) calculations. The interconversion of Pd_2L_4 and PdL_2 can be achieved *via* the *cis-trans* isomerization of the azobenzene unit on the ligand upon alternative irradiation of light 365 nm or 420 nm.

© 2023 Published by Elsevier B.V. on behalf of Chinese Chemical Society and Institute of Materia Medica, Chinese Academy of Medical Sciences.

Stimuli-responsive self-assembled systems have important value in the application of mimics of dynamic biosystems [1,2], constructions of molecular machines [3–5] and fabrications of smart materials [6–9]. Stimuli-responsive metal-organic cages whose structures can be changed to affect host-guest binding properties, thus achieving controlled encapsulation and release of guests, are receiving increasing attention. Various stimuli have been exploited to regulate the metal-organic cages, such as light [10,11], pH [12–14], solvent [15,16], temperature [17,18], electric potential [19,20], or ion [21–24]. Among these, light is highly advantageous because it can be used with high spatial and temporal precision and without waste generation.

The development of light-responsive metal-organic cages remains challenging because the total number of successful examples is limited [25]. So far, two types of light-responsive metal-organic cages have been reported, one is that light-responsive units are dangled on the cages [26–28], and the other is that photoswitchable units serve as the integral part of the cage backbone, causing disassembly/reassembly [29,30], deformation [31–33] and interconversion between different assemblies [34–37]. Photoswitches can be used to modulate the structures of metal-assemblies, but they usually lead to the formation of non-discrete structures [38,39]. So far, there is still few related reports on realizing light-driven interconversion of discrete metal-assemblies. For example, the open- and closed-diarylethene were used to achieve the interconversion of Pd_3L_6 and $Pd_{24}L_{48}$ [34,35], and the light-driven switching between cage Pd_2L_4 and bowl Pd_2L_3 [36]. Another recent work on visible-light-driven Pd_2L_4 and PdL_2 interconversion based on azobenzene ligand [37] was published during our preparation of this manuscript. Therefore, it is of significant scientific value to develop a light-responsive system that maintains discrete structures.

Herein, a bis-pyridyl ligand containing an azobenzene backbone with two picolyls attached at both ends–(*E*)-1,2-bis(4-(pyridin-3-ylmethyl)phenyl)diazene (***trans*-L**)—was designed and synthesized. When coordinated with Pd^{2+}, ***trans*-L** leads to the formation of lantern-shaped cage $[Pd_2(\textbf{\textit{trans}-L})_4]^{4+}$, while the *cis*-isomer (***cis*-L**) forms tweezer-like $[Pd(\textbf{\textit{cis}-L})_2]^{2+}$. The interconversion of the two different discrete self-assemblies can be realized *via* the isomerization of **L** under alternative irradiation of 365 nm or 420 nm light (Fig. 1).

The free ligand ***trans*-L** was synthesized by the oxidation of 4-(pyridin-3-ylmethyl)aniline (Scheme S1 in Supporting information) and its photoisomerization behavior was first investigated by ^1H NMR spectroscopy. The complete ^1H resonance assignments of ***trans*-L** and ***cis*-L** were based on their chemical shifts, ratios of integral areas, coupling constants (Fig. 2 and Schemes S1 and S2 in Supporting information) and the cross peaks in the ^1H-^1H COSY NMR spectrum (Figs. S5 and S8 in Supporting information). Upon the irradiation of ***trans*-L** in CD_3CN at 365 nm for 5 min, it reached a photostationary state comprising of 94% ***cis*-L** (Fig. 2b). When the resulting solution was subsequently irradiated with 420 nm light

* Corresponding author.
E-mail address: qcwang@ecust.edu.cn (Q. Wang).

https://doi.org/10.1016/j.cclet.2022.108002
1001-8417/© 2023 Published by Elsevier B.V. on behalf of Chinese Chemical Society and Institute of Materia Medica, Chinese Academy of Medical Sciences.

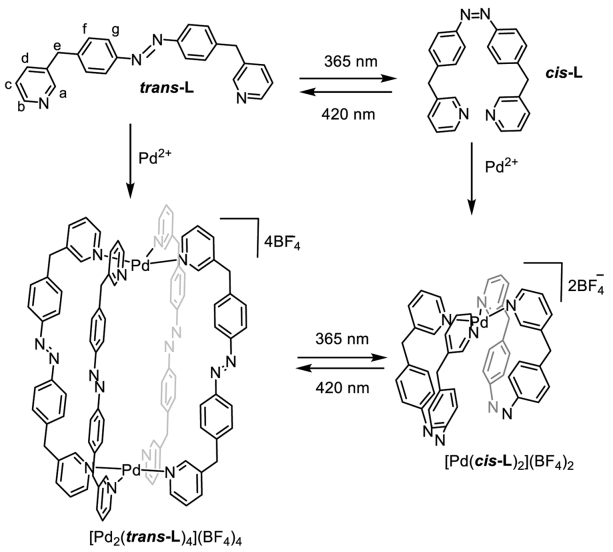

Fig. 1. Schematic diagram of the light-driven interconversion of **L** and its Pd^{2+} self-assemblies.

for 5 min, ***cis*-L** was found to be switched back to ***trans*-L** with a new photostationary state containing 77% ***trans*-L** (Fig. 2c). When compared with those of ***trans*-L**, the protons on the azobenzene units (H_g and H_f) of ***cis*-L** shift upfield ($\Delta\delta_{Hg} = -1.06$ ppm and $\Delta\delta_{Hf} = -0.29$ ppm) due to encountering additional shielding effect of the remote out-of-plane aromatic ring (*cis*) [40]. The UV-vis absorption spectroscopy was also exploited to monitor the photoisomerization between ***trans*-L** and ***cis*-L** in acetonitrile. As illustrated in Fig. 2d, ***trans*-L** has a strong absorption band at 335 nm and a weak one at 430 nm assigned to its π-π^* and n-π^* excitation, respectively. Irradiation of ***trans*-L** with UV light leads to the decrease of absorption intensity at 335 and the increase at 430 nm, indicating the conversion from ***trans*-L** to ***cis*-L**. The reversed conversion was verified by the increase in absorption intensity at 335 nm and decrease at 430 nm after subsequent irradiation at 420 nm, and the isosbestic points for this isomerization process appeared at 285 and 390 nm. The thermal half-time of the switchable ligand **L** was measured as 83 h at 298 K from UV-vis spectra (Figs. S21 and S22 in Supporting information). Furthermore, by alternating irradiation of the ligand **L** with light of 365 or 420 nm for 30 cycles, the absorption intensity of **L** at 335 nm was monitored to perform a regular fluctuation, with slight change under the same light irradiation, indicating that it has good reversible photoisomerization (Fig. S23 in Supporting information).

The Pd-based assembly of ***trans*-L** was subsequently investigated. Mixing ***trans*-L** with $[Pd(CH_3CN)_4](BF_4)_2$ in 2:1 molar ratios in CD_3CN at 70 °C for 5 h led to the formation of a new coordination species, which was characterized by ^1H NMR spectroscopy (Fig. 3a, Fig. S9 and Scheme S3 in Supporting information). The ^1H NMR signals of the form species were also attributed by the ^1H-^1H COSY NMR spectroscopy (Fig. S12 in Supporting information). Compared with the free ***trans*-L**, most of the proton signals on pyridine of this new species shift downfield ($\Delta\delta_{Hb} = +0.23$ ppm, $\Delta\delta_{Hc} = +0.30$ ppm and $\Delta\delta_{Hd} = +0.41$ ppm), indicating the coordination with electron-withdrawing Pd^{2+} ion (Figs. 3a and b). However, H_a was found upfiled-shifting ($\Delta\delta_{Ha} = -0.57$ ppm), which suggests that except the deshielding effects from the coordination Pd^{2+}, H_a must bear a strong shielding effect from the newly formed assembly, as observed in other Pd-based molecular cages [10,41,42]. High resolution ESI-MS spectroscopy confirms this species as $[Pd_2(\textbf{\textit{trans}-L})_4](BF_4)_4$ cage. The MS signal peaks of *trans*-species appeared at *m/z* 417.8626, 585.8291, 922.2343, assigned to $[Pd_2(\textbf{\textit{trans}-L})_4]^{4+}$, $[Pd_2(\textbf{\textit{trans}-L})_4+BF_4]^{3+}$, $[Pd_2(\textbf{\textit{trans}-L})_4+2BF_4]^{2+}$, respectively (Fig. 3f and Fig. S13 in Supporting information). And the resolved peaks appear with differences of 0.25, 0.33, 0.50, respectively, which are consistent with the simulated values, further confirming the composition of the coordination species (Fig. S14 in Supporting information).

The photoisomerization behavior of $[Pd_2(\textbf{\textit{trans}-L})_4](BF_4)_4$ in CD_3CN was first irradiated at 365 nm for 20 min and then characterized by ^1H NMR. The signals of $[Pd_2(\textbf{\textit{trans}-L})_4](BF_4)_4$ disappear and a new single set of peaks originates, accompanied with the significant upfield shifted H_f and H_g signals ($\Delta\delta_{Hg} = -1.30$ ppm and $\Delta\delta_{Hf} = -0.33$ ppm), suggesting the formation of a new discrete complex containing ***cis*-L**. The ^1H NMR peaks of this *cis*-complex were assigned under the assistance of COSY NMR (Fig. S18 in Supporting information). The pyridine protons (H_b, H_c and H_d) of this *cis*-complex were found again downfield shifted ($\Delta\delta_{Hb} = +0.46$ ppm, $\Delta\delta_{Hc} = +0.27$ ppm and $\Delta\delta_{Hd} = +0.39$ ppm) when compared with the free ligand ***cis*-L** (Figs. 3c and d), confirming that the pyridine unit still coordinates with Pd^{2+}. However, the change of the chemical shifts of H_a ($\Delta\delta_{Ha} = +0.05$ ppm) is quite different from that of the above *trans*-cage ($\Delta\delta_{Ha} = -0.57$ ppm), indicating that H_a of this *cis*-complex undergoes weaker shielding effects than that of the *trans*-cage. These results suggest the formation of a new $Pd_n(\textbf{\textit{cis}-L})_{2n}$ assembly [43,44] rather than $Pd_2(\textbf{\textit{cis}-L})_4$. Further high resolution ESI-MS spectra show that two sets of peaks appeared at *m/z* 417.1156 and 921.2427, and their resolved peaks appear with differences of 0.5, 1.0, which are consistent with the simulated values of $[PdC_{48}H_{40}N_8]^{2+}$ and $[PdC_{48}H_{40}N_8BF_4]^+$, respectively (Fig. 3g and Fig. S19 in Supporting information). All these results demonstrate that the *cis*-species is $[Pd(\textbf{\textit{cis}-L})_2](BF_4)_2$, which can also be synthesized *via* the coordination of ***cis*-L** with $[Pd(CH_3CN)_4](BF_4)_2$

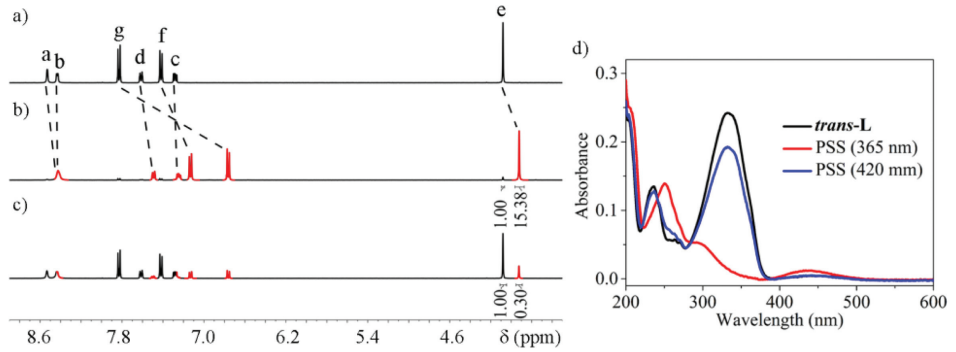

Fig. 2. ^1H NMR (400 MHz, CD_3CN) spectra of (a) ***trans*-L**, (b) the irradiation of the solution (a) at 365 nm for 5 min, (c) the irradiation of the solution (b) at 420 nm for 5 min (black represents ***trans*-L** and red represents ***cis*-L**). (d) UV-vis absorption spectra of **L**.

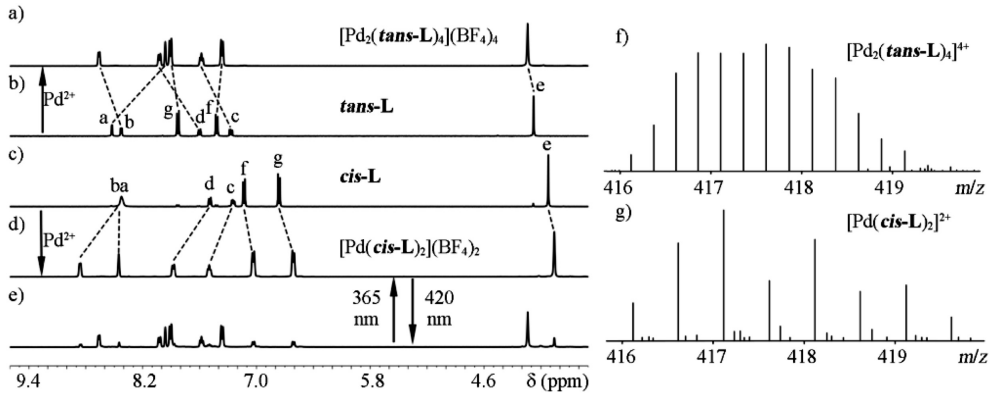

Fig. 3. ^{1}H NMR (400 MHz, CD_3CN) spectra of: (a) $[Pd_2(\textbf{\textit{trans}}\text{-L})_4](BF_4)_4$, (b) ***trans*-L**, (c) ***cis*-L**, (d) $[Pd_2(\textbf{\textit{cis}}\text{-L})_2](BF_4)_2$, (e) the irradiation of $[Pd_2(\textbf{\textit{cis}}\text{-L})_2](BF_4)_2$ at 420 nm for 20 min. High resolution ESI-MS spectra of (f) $[Pd_2(\textbf{\textit{trans}}\text{-L})_4](BF_4)_4$ and (g) $[Pd(\textbf{\textit{cis}}\text{-L})_2](BF_4)_2$.

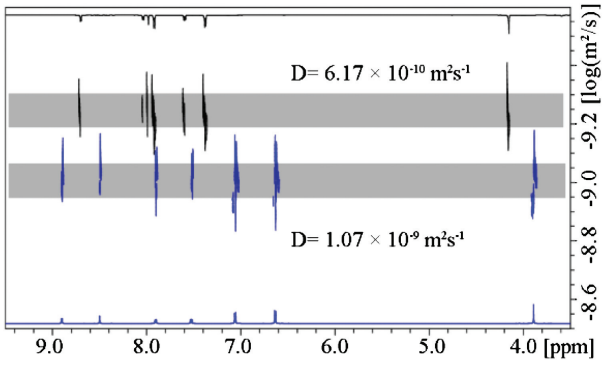

Fig. 4. Overlaid ^{1}H DOSY NMR (600 MHz, CD_3CN) spectra of $[Pd_2(\textbf{\textit{trans}}\text{-L})_4](BF_4)_4$ and $[Pd(\textbf{\textit{cis}}\text{-L})_2](BF_4)_2$ (black represents $Pd_2(\textbf{\textit{trans}}\text{-L})_4](BF_4)_4$, and blue represents $[Pd(\textbf{\textit{cis}}\text{-L})_2](BF_4)_2$).

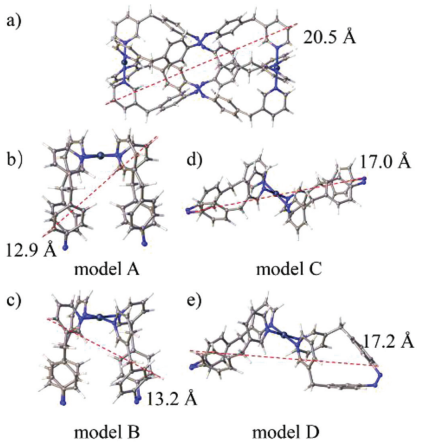

Fig. 5. DFT-optimized structure and the longest diameter calculated for (a) $[Pd_2(\textbf{\textit{trans}}\text{-L})_4](BF_4)_4$ and (b) model A of $[Pd(\textbf{\textit{cis}}\text{-L})_2](BF_4)_2$, (c) model B of $[Pd(\textbf{\textit{cis}}\text{-L})_2](BF_4)_2$, (d) model C of $[Pd(\textbf{\textit{cis}}\text{-L})_2](BF_4)_2$, (e) model D of $[Pd(\textbf{\textit{cis}}\text{-L})_2](BF_4)_2$.

(Scheme S4 in Supporting information). Furthermore, all NMR peaks of $[Pd_2(\textbf{\textit{trans}}\text{-L})_4](BF_4)_4$ and $[Pd(\textbf{\textit{cis}}\text{-L})_2](BF_4)_2$ remain sharp without splitting and no miscellaneous peaks appear, which indicates that the two species are symmetrical discrete palladium-based coordination compounds in regard to the NMR timescale.

^{1}H Diffusion-ordered NMR spectroscopies (DOSY) were also conducted for the characterization of the two discrete coordination assemblies [45]. The diffusion coefficients (D) of $[Pd_2(\textbf{\textit{trans}}\text{-L})_4](BF_4)_4$ and $[Pd(\textbf{\textit{cis}}\text{-L})_2](BF_4)_2$) were measured as 6.17×10^{-10} and 1.07×10^{-9} m^2/s in CD_3CN (Fig. 4, Figs. S11 and S17 in Supporting information), and the hydrodynamic radiuses are calculated as 9.6 Å and 5.5 Å, respectively, according to Stokes-Einstein equation.

In general, the fine structure of coordination compound is intuitively provided by X-ray single crystal diffraction. However, both crystals of $[Pd_2(\textbf{\textit{trans}}\text{-L})_4](BF_4)_4$ and $[Pd(\textbf{\textit{cis}}\text{-L})_2](BF_4)_2$ were not obtained after numerous attempts. Therefore, the theoretical structures of the two assemblies were determined by density function theory (DFT) geometry optimization. As shown in Fig. 5a and Fig. S28 (Supporting information), $[Pd_2(\textbf{\textit{trans}}\text{-L})_4](BF_4)_4$ features typical lantern-shaped structure with four twisted ligands and has a cavity with the distance of Pd to Pd being 15.1 Å. The longest outer diameter is 20.5 Å, which is well-matched with the hydrodynamic diameter measured from ^{1}H DOSY experiment ($2r = 2 \times 9.6$ Å $= 19.2$ Å). Moreover, four possible isomers of $[Pd(\textbf{\textit{cis}}\text{-L})_2](BF_4)_2$ appear with energy difference within 3 kcal/mol (Figs. 5b-e, Fig. S29 and Table S1 in Supporting information) and the longest outer diameters were calculated as 12.9 Å, 13.2 Å, 17.0 Å and 17.2 Å in model A, model B, model C and model D, respectively. Considering that the calculated molecular diameter should be consistent with the hydrodynamic diameter ($2r = 2 \times 5.5$ Å $= 11.0$ Å), $[Pd(\textbf{\textit{cis}}\text{-L})_2](BF_4)_2$ is visualized as a tweezer-like structure with two ***cis*-L** on the same side of Pd (model A and model B). And it is assumed to be a mixture of two stereoisomers being in fast exchange with respect to the NMR timescale due to the similar energies of the structures of model A and model B ($\Delta E = 0.05$ kcal/mol). Since the process of de- and re-coordination of the pyridine ligands to the palladium cations needs minute-scale time to complete in CH_3CN at room temperature [46], the equilibration is speculated to take place by the rotations around the C-N and -CH_2- bonds in $[Pd(\textbf{\textit{cis}}\text{-L})_2](BF_4)_2$ (Scheme S4).

The reverse process was also investigated by the irradiation of $[Pd(\textbf{\textit{cis}}\text{-L})_2](BF_4)_2$ with 420 nm light for 20 min. The ^{1}H NMR spectra show that the intensity of the peaks corresponding to $[Pd(\textbf{\textit{cis}}\text{-L})_2](BF_4)_2$ decrease and the signals for $[Pd_2(\textbf{\textit{trans}}\text{-L})_4](BF_4)_4$ appear, indicating $[Pd(\textbf{\textit{cis}}\text{-L})_2](BF_4)_2$ again is converted to $[Pd_2(\textbf{\textit{trans}}\text{-L})_4](BF_4)_4$ in a 75% conversion efficiency according to the NMR integration (Fig. 3e and Fig. S25 in Supporting information). Moreover, the two Pd-based species exhibit good reversibility induced by switching light of 365 nm and 420 nm (Figs. S24 and S27 in Supporting information). The conversion of $[Pd_2(\textbf{\textit{trans}}\text{-L})_4](BF_4)_4$ and $[Pd(\textbf{\textit{cis}}\text{-L})_2](BF_4)_2$ was also investigated by UV-vis absorption spectroscopy with different irradiation time (Figs. S26 in Supporting information). The absence of isosbestic points indicates that the presence of other process besides the isomerization of

azobenzene, which is considered to be the coordination and de-coordination of pyridine with Pd^{2+}.

In conclusion, a light-switchable Pd_nL_{2n} (n = 1 or 2) self-assembly system based on azobenzene-containing ligands was reported. The lantern-shaped cage Pd_2L_4 and the tweezer-like PdL_2 were synthesized individually by coordination of palladium ion with ***trans*-L** or ***cis*-L**, respectively. And the two discrete coordination species can also be converted into each other by switching the light source of 365 nm or 420 nm. This system undergoes major structural changes and has potential applications as smart materials such as releasing loaded drugs.

Declaration of competing interest

The authors declare that they have no known competing financial interests or personal relationships that could have appeared to influence the work reported in this paper.

Acknowledgments

This work was financially supported by the National Natural Science Foundation of China (No. 21572063), Shanghai Municipal Science and Technology Major Project (No. 2018SHZDZX03) and the Fundamental Research Funds for the Central Universities.

Supplementary materials

Supplementary material associated with this article can be found, in the online version, at doi:10.1016/j.cclet.2022.108002.

References

[1] A. Sikder, C. Esen, R.K. O'Reilly, Acc. Chem. Res. 55 (2022) 1609–1619.
[2] W. Li, Z. Yan, J. Ren, X. Qu, Chem. Soc. Rev. 47 (2018) 8639–8684.
[3] I. Neira, A. Blanco-Gomez, J.M. Quintela, et al., Acc. Chem. Res. 53 (2020) 2336–2346.
[4] J. Wankar, N.G. Kotla, S. Gera, et al., Adv. Funct. Mater. 30 (2020) 1909049.
[5] Y. Wu, L. Shangguan, Q. Li, et al., Angew. Chem. Int. Ed. 60 (2021) 19997–20002.
[6] Q. Wang, C. Wang, S. Li, et al., Chem. Mater. 34 (2022) 2085–2097.
[7] E. Moulin, L. Faour, C.C. Carmona-Vargas, N. Giuseppone, Adv. Mater. 32 (2020) 1906036.
[8] Y. Wang, J. Gong, X. Wang, et al., Angew. Chem. Int. Ed. 61 (2022) e202210542.
[9] W. Zhang, Y. Luo, X.L. Ni, et al., Chem. Eng. J. 446 (2022) 136954.
[10] M. Han, R. Michel, B. He, et al., Angew. Chem. Int. Ed. 52 (2013) 1319–1323.
[11] R.J. Li, J.J. Holstein, W.G. Hiller, et al., J. Am. Chem. Soc. 141 (2019) 2097–2103.
[12] L. Xu, D. Zhang, T.K. Ronson, J.R. Nitschke, Angew. Chem. Int. Ed. 59 (2020) 7435–7438.
[13] S.M. Jansze, G. Cecot, K. Severin, Chem. Sci. 9 (2018) 4253–4257.
[14] S.M. Jansze, K. Severin, J. Am. Chem. Soc. 141 (2019) 815–819.
[15] L.X. Cai, D.N. Yan, P.M. Cheng, et al., J. Am. Chem. Soc. 143 (2021) 2016–2024.
[16] Y. Wang, Y. Zhang, Z. Zhou, et al., Nat Commun. 11 (2020) 2727.
[17] D. Zhang, T.K. Ronson, S. Guryel, et al., J. Am. Chem. Soc. 141 (2019) 14534–14538.
[18] S.G. Chen, Z.X. Zhao, X.N. Jiang, et al., Chem Asian J. 11 (2016) 465–469.
[19] V. Croue, S. Goeb, G. Szaloki, et al., Angew. Chem. Int. Ed. 55 (2016) 1746–1750.
[20] R.A.S. Vasdev, J.A. Findlay, A.L. Garden, J.D. Crowley, Chem. Commun. 55 (2019) 7506–7509.
[21] S. Sudan, F. Fadaei-Tirani, R. Scopelliti, et al., Angew. Chem. Int. Ed. 61 (2022) e202201823.
[22] D. Preston, A. Fox-Charles, W.K.C. Lo, J.D. Crowley, Chem. Commun. 51 (2015) 9042–9045.
[23] A.P. Birve, H.D. Patel, J.R. Price, et al., Angew. Chem. Int. Ed. 61 (2022) e202115468.
[24] D. Ogata, J. Yuasa, Angew. Chem. Int. Ed. 58 (2019) 18424–18428.
[25] S.J. Wezenberg, Chem. Lett. 49 (2020) 609–615.
[26] Y. Jiang, J. Park, P. Tan, et al., J. Am. Chem. Soc. 141 (2019) 8221–8227.
[27] T. Murase, S. Sato, M. Fujita, Angew. Chem. Int. Ed. 46 (2007) 5133–5136.
[28] J. Park, L.B. Sun, Y.P. Chen, et al., Angew. Chem. Int. Ed. 53 (2014) 5842–5846.
[29] S. Fu, Q. Luo, M. Zang, et al., Materials Chem. Front. 3 (2019) 1238–1243.
[30] R.J. Li, C. Pezzato, C. Berton, K. Severin, Chem. Sci. 12 (2021) 4981–4984.
[31] S. Oldknow, D.R. Martir, V.E. Pritchard, et al., Chem. Sci. 9 (2018) 8150–8159.
[32] C. Stuckhardt, D. Roke, W. Danowski, et al., Beilstein J. Org. Chem. 15 (2019) 2767–2773.
[33] H. Lee, J. Tessarolo, D. Langbehn, et al., J. Am. Chem. Soc. 144 (2022) 3099–3105.
[34] Y. Gu, E.A. Alt, H. Wang, et al., Nature 560 (2018) 65–69.
[35] M. Han, Y. Luo, B. Damaschke, et al., Angew. Chem. Int. Ed. 55 (2016) 445–449.
[36] R.J. Li, J. Tessarolo, H. Lee, G.H. Clever, J. Am. Chem. Soc. 143 (2021) 3865–3873.
[37] R.G. DiNardi, A.O. Douglas, R. Tian, et al., Angew. Chem. Int. Ed. 61 (2022) e202205701.
[38] A.D.W. Kennedy, R.G. DiNardi, L.L. Fillbrook, et al., Chem. Eur. J. 28 (2022) e202104461.
[39] X. Yan, J.F. Xu, T.R. Cook, et al., Proc. Natl. Acad. Sci. U. S. A. 111 (2014) 8717–8722.
[40] K.M. Tait, J.A. Parkinson, S.P. Bates, et al., J. Photoch. Photobio. A 154 (2003) 179–188.
[41] J. Zhu, C. Li, X. Li, et al., Chin. Chem. Lett. 34 (2023) 107693.
[42] M. Yamashina, T. Yuki, Y. Sei, et al., Chem. Eur. J. 21 (2015) 4200–4204.
[43] S. Bandi, S. Samantray, R.D. Chakravarthy, et al., Eur. J. Inorg. Chem. 2016 (2016) 2816–2827.
[44] D.A. McMorran, P.J. Steel, Supramol. Chem. 14 (2010) 79–85.
[45] L. Avram, Y. Cohen, Chem. Soc. Rev. 44 (2015) 586–602.
[46] G.H. Clever, M. Shionoya, Chem. Eur. J. 16 (2010) 11792–11796.